

Numerical simulation of the localization of elastic waves in two- and three-dimensional heterogeneous media

Reza Sepehrinia¹, M. Reza Rahimi Tabar^{1,2}, and Muhammad Sahimi^{3,*}

¹*Department of Physics, Sharif University of Technology, Tehran 11155-9161, Iran*

²*Institute of Physics, Carl von Ossietzky University, Oldenburg D-26111, Germany*

³*Mork Family Department of Chemical Engineering & Materials Science, University of Southern California, Los Angeles, California 90089-1211, USA*

Localization of elastic waves in two-dimensional (2D) and three-dimensional (3D) media with random distributions of the Lamé coefficients (the shear and bulk moduli) is studied, using extensive numerical simulations. We compute the frequency-dependence of the minimum positive Lyapunov exponent γ (the inverse of the localization length) using the transfer-matrix method, the density of states utilizing the force-oscillator method, and the energy-level statistics of the media. The results indicate that all the states may be localized in the 2D media, up to the disorder width and the smallest frequencies considered, although the numerical results also hint at the possibility that there might a small range of the allowed frequencies over which a mobility edge might exist. In the 3D media, however, most of the states are extended, with only a small part of the spectrum in the upper band tail that contains localized states, even if the Lamé coefficients are randomly distributed. Thus, the 3D heterogeneous media still possess a mobility edge. If both Lamé coefficients vary spatially in the 3D medium, the localization length Λ follows a power law near the mobility edge, $\Lambda \sim (\Omega - \Omega_c)^{-\nu}$, where Ω_c is the critical frequency. The numerical simulation yields, $\nu \simeq 1.89 \pm 0.17$, significantly larger than the numerical estimate, $\nu \simeq 1.57 \pm 0.01$, and $\nu = 3/2$, which was recently derived by a semiclassical theory for the 3D Anderson model of electron localization. If the shear modulus is constant but the bulk modulus varies spatially, the plane waves with transverse polarization propagate without any scattering, leading to a band of completely extended states, even in the 2D media. At the mobility edge of such media the localization length follows the same type of power law as Λ , but with an exponent, $\nu_T \simeq 1/2$, for both 2D and 3D media.

PACS numbers: 62.30.+d, 05.10.Cc, 71.23.An

I. INTRODUCTION

Propagation of elastic waves in random media has been a subject of much interest for several decades. The reason for the interest is at least twofold. One is that propagation of elastic waves in rock provides much information on its structure and content.^{1,2} For example, seismic wave propagation and reflection are used for not only estimating the hydrocarbon contents of an oil or natural gas reservoir, but also obtaining information on the spatial distributions of the reservoir's fractures, faults, and strata, as well as its porosity. They are also the main tool for imaging rock structure over a wide area, ranging from the Earth's near surface to the deeper crust and upper mantle. How the inhomogeneities within the Earth's crust affect propagation of elastic waves has also been, for a long time, a subject of much interest.³ Other rock-related phenomena and problems in which propagation of elastic waves plays a significant, and often fundamental, role include the analysis of seismic records for earthquakes in order to develop a theory for predicting when and where an earthquake may occur,⁴ and detecting underground nuclear explosions.

The second reason for the interest in understanding elastic wave propagation is related to the characterization of materials, the effect of heterogeneities on their macroscopic properties, and development of a link between their static and dynamical properties.⁵ This prob-

lem has also been studied for several decades.⁶ In particular, propagation of elastic waves has been a major tool for nondestructive evaluation of composite materials, and gauging the effect that the defects have on their properties.^{5,7}

As elastic waves propagate in a disordered material, the heterogeneities cause multiple scattering of, and interference in, the waves. The scattering process modifies both the travel time and amplitudes of the propagating waves. An important question, then, is whether the heterogeneities and the associated scattering and interference phenomena can give rise to *localization* of the elastic waves. By localization, we mean a phenomenon in which, over finite lengths scales (which could, however, be quite large), a wave's amplitude decays and eventually vanishes. It was recently reported,⁸ through elegant experiments, that seismic waves propagating in rock samples exhibit *weak* localization. The fundamental mechanism for weak localization is *constructive interference* of an incident beam, travelling in a given scattering path, and the waves that move along the same path in the backscattering direction. Constructive interference exists only in a narrow range of the angles around the backscattering direction. The typical width of the cone is of the order of ζ/ℓ , where ζ is the wavelength and ℓ the mean-free path of the waves. Thus, for a medium with a high density of the scatterers, the backscattering cone is wider. Indeed, the criterion for the existence of the weak localization

regime is, $\zeta/\ell \gg 1$. Weak localization is also important due to it being a precursor to the strong localization, which is also the result of multiple scattering by a spatial distribution of scatterers. As is well known, the main consequence of strong localization is the absence of diffusion of waves over length scales that are larger than the localization length.⁹

Localization of elastic waves in disordered media have important practical implications. Consider, as an example, propagation of elastic waves in rock. If the waves do localize, then, their scattering and reflection by the rock can provide useful information on its structure only over length scales that are on the order of the localization length of the waves, or smaller. Thus, if, for example, a station that records information on the seismic waves that emanate from an earthquake epicenter is farther from the center than the localization length of the waves, the records cannot provide much useful information on the phenomena that led to the earthquake and its aftermath.

A very useful quantity for determining whether a state is delocalized or localized is the minimum positive Lyapunov exponent γ , which is simply the inverse of the localization length ξ . If $\gamma > 0$ for all the energies or frequencies ω , then, all the states are localized; that is, the wave function $\psi(r)$ decays at large distances r from the center of the material's domain as, $\psi(r) \sim \exp[-\gamma(\omega)r]$. Another useful property is the vibrational density of states of disordered elastic materials, which depends strongly on the strength of the disorder in the materials.

In the present paper we carry out extensive numerical simulations in order to study the frequency-dependence of several properties of disordered elastic media in both two- and three-dimensional (3D) media, and investigate the conditions under which elastic waves in such media may become localized. We compute the localization properties of disordered elastic media as a function of the frequency using the transfer-matrix method. In particular we compute the frequency-dependence of the minimum positive Lyapunov exponent near the localization-delocalization transition. The frequency-dependent properties that we study also include the statistics of the energy levels and the distribution of the spacings (gaps) between the nearest-neighbor levels. The distribution of the level spacings for certain matrices has been studied through the theory of random matrices.^{10,11} It has been shown that the statistics of the energy levels in the metallic regime of the Anderson localization⁹ follow the well-known Wigner-Dyson statistics.¹⁰ The symmetries of the Hamiltonian that describe a phenomenon in a disordered medium affect the universality class of the transition and the distribution function of the level spacings. Therefore, it should be interesting, as well as important, to study whether the statistics that we compute for elastic waves in disordered media fall in any known universality class, such as that of the Anderson model, or that they give rise to a new

class.

To carry out the numerical simulations, we consider a medium with a constant density and continuous spatial distributions of the Lamé coefficients. The governing equations for the propagation of elastic waves in such a medium are then discretized and solved. The discretization does, of course, introduce a cutoff length scale into the problem, namely, the lattice spacing or the linear size of the blocks in the computational grid. Thus, the results are valid for the wavelengths that are larger than the basic linear size of the blocks. At the same time, though, the model that we study is one that has been used extensively in the geophysics literature for representing the propagation of seismic waves. Thus, our results are directly relevant to seismic wave propagation in heterogeneous rock.

In addition to the above considerations, the present study is also motivated by, and represents a continuation of, our recent study¹² of propagation of elastic waves in 2D disordered media. In that study the Martin-Siggia-Rose method¹³ was used, and the one-loop dynamic renormalization group (RG) equations were derived for the coupling constants, in the limit of low frequencies (long wavelengths). The RG analysis made it possible to identify those regions in the coupling constants space in which the elastic waves are localized or extended. Thus, using extensive numerical simulations, we aim in the present paper to check the predictions of the RG analysis carried out previously.¹² In addition, our work is relevant to phonon localization in disordered solids that has been studied extensively in the past. Such a phenomenon has been studied classically, using both the scalar and vector models of vibrations in disordered materials,^{14–16} although the vector models used previously are different from what we consider in the present paper.

The rest of this paper is organized as follows. In the next section we describe the model of the heterogeneous elastic media and the governing equations for elastic wave propagation in such media that we study in this paper. Section III describes the transfer-matrix computation of the Lyapunov exponents, while the calculation of the density of states is described in Sec. IV. The results are presented and discussed in Sec. V, while Sec. VI summarizes the paper.

II. MODEL AND GOVERNING EQUATIONS

Many of the theoretical studies of wave propagation in heterogeneous media (such as rock) are based on the elastic wave equation

$$m \frac{\partial^2 u_i}{\partial t^2} = \partial_j \sigma_{ij} , \quad (1)$$

which represents the equation of motion for an elastic medium with mean density m . Here, u_i is the displacement in the i th direction, σ_{ij} the ij th component of the stress tensor σ , and t is the time. As usual, σ_{ij} is written

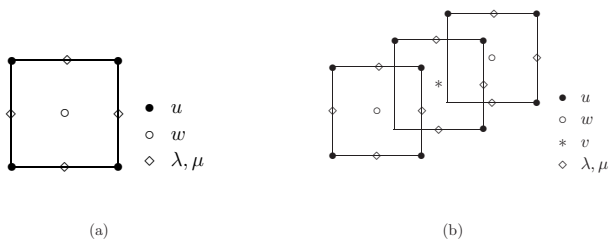


FIG. 1: (a) Two- and (b) three-dimensional staggered grids used in the simulations. Symbols on the grid blocks indicate the grid points at which the associated quantities are evaluated.

in terms of the strain tensor,

$$\sigma_{ij} = 2\mu(\mathbf{x})u_{ij} + \lambda(\mathbf{x})u_{kk}\delta_{ij}, \quad (2)$$

where u_{ij} is ij component of the the strain tensor, and $\mu(\mathbf{x})$ and $\lambda(\mathbf{x})$ are the spatially-varying Lamé coefficients. For small deformations of the medium the strain tensor has the following linear form in terms of the displacement components u_i and u_j ,

$$u_{ij} = \frac{1}{2}(\partial_i u_j + \partial_j u_i). \quad (3)$$

In the computer simulations that are described below we take the Lamé coefficients λ and μ to be uniformly distributed in the intervals $[\lambda_0 - W_\lambda, \lambda_0 + W_\lambda]$, and $[\mu_0 - W_\mu, \mu_0 + W_\mu]$, where λ_0 and μ_0 are the mean values of the coefficients.

Accurate numerical simulation of Eq. (1) [together with Eqs. (2) and (3)] is difficult, particularly if one solves it for a heterogeneous medium in which the Lamé coefficients vary spatially. There have been many attempts in the geophysics literature to solve Eq. (1) numerically in the time domain,^{17–20} using a variety of schemes and computational grids. Typically, in these works,^{17–20} Eq. (1) was discretized by the finite-difference (FD) technique. However, use of the central-difference FD method, together with cubic computational grids, can give rise to certain instabilities in the solution. It has been shown²¹ that stable numerical solutions are obtained if one uses a staggered computational grid, in order to define the variables and discretize Eq. (1), unless the medium contains singularities (such as cracks) or free surfaces, in which case a rotated staggered grid may be more appropriate.

In the present study we used the staggered computational grids, shown in Fig. 1, in the numerical simulations of Eq. (1). Discretizing Eq. (1) on such a grid leads to a symmetric Hamiltonian, as expected. We then seek monochromatic solutions of Eq. (1) for a given frequency, in the form, $u_i(\mathbf{x}, t) = u_i(\mathbf{x}) \exp(i\omega t)$. Writing, $\mathbf{u} = (u, w)$ in 2D and, $\mathbf{u} = (u, w, v)$ in 3D, and discretizing Eq. (1) by the FD method on the staggered grid shown in Fig. 1, we obtain a set of discretized equations for the determination of the monochromatic solutions.

The resulting discretized equations are given in the Appendix.

The problem of solving the set of the discretized equations, Eqs. (A1), (A2), and (A5) - (A7) of the Appendix is then formulated as one of an eigenvalue problem. If we define a vector \mathbf{Z} , the components of which represent all the field variables (displacements) at the grid points, then the set of the discretized equations is written as

$$\sum_{\beta} H_{\alpha\beta} Z_{\beta} = \Omega Z_{\alpha}, \quad (4)$$

where, $\Omega = \omega^2$, with the matrix of the coefficients \mathbf{H} being symmetric. As mentioned above, discretizing the governing equations introduces a cutoff length scale and, hence, a cutoff frequency in the simulations, which do not exist in the continuum equations (1). We neglect such difference between the discrete and continuous system (which can be reduced by decreasing the size of the blocks in the computational grid).

III. TRANSFER-MATRIX CALCULATIONS

To determine whether an eigenstate is localized or extended in the thermodynamic (large system size) limit, we calculate the minimum positive Lyapunov exponent γ_m , which is simply the inverse of the localization length. The most suitable numerical method for directly computing the localization properties of noninteracting disordered media is, perhaps, the transfer-matrix (TM) technique, using a strip (bar) in two (three) dimensions, with periodic boundary conditions in the transverse direction(s). To formulate the TM computations, we rewrite the difference Eqs. (A1), (A2), and (A5) - (A7) in the following form

$$\begin{pmatrix} \mathbf{Z}_{n+1} \\ \mathbf{Z}_n \end{pmatrix} = \mathbf{T}_n \begin{pmatrix} \mathbf{Z}_n \\ \mathbf{Z}_{n-1} \end{pmatrix}, \quad (5)$$

where \mathbf{Z}_n is the vector that contains the values of (the discretized) displacements $\mathbf{u}(\mathbf{x})$ in slice number n in the 2D strip or the 3D bar. For 2D media, for example, \mathbf{Z}_n contains $2M$ components because every grid point is characterized by two displacements (u, w) (see Fig. 1). Thus, the vectors on both sides of Eq. (5) contain $4M$ components and, as a result, \mathbf{T}_n is a $4M \times 4M$ matrix, resulting in $4M$ Lyapunov exponents, half ($2M$) of which are independent as they appear in pairs, $(\gamma, -\gamma)$.

Because the discretized equations are defined on a staggered grid (Fig. 1), and we have a set of coupled equations for each grid points, instead of a single equation (because we solve a vector equation), the slices for the TM steps should be defined carefully. In 2D we impose the boundary condition on one side of the strip and then move forward in the (longitudinal) x direction by multiplication of the TM matrices. To do this, we define the set of two lines, $x = i$ and $x = i + \frac{1}{2}$, as a single slice. All the variables in the slice $(i + 1, i + 1 + \frac{1}{2})$ are then computed, if one knows the values in the slices $(i, i + \frac{1}{2})$ and

$(i-1, i-1 + \frac{1}{2})$. In the same way, a boundary condition is imposed on one end plane of the bar, and a 3D slice is defined as being composed of two planes, $z = k$ and $z = k + \frac{1}{2}$.

We used $M \times L$ strips and $M \times M \times L$ bars, where M is the transverse dimension, and L the length. If $N = dM^{d-1}$, where $d = 2$ and 3 , then, the dimensions of the TM in Eq. (5) and number of the Lyapunov exponents are $2N$. Therefore, the simulations start with $2N$ initial orthonormal vectors, corresponding to the dimension of the TM, taken to be, $\mathbf{v} = (1, 0, \dots, 0)^T$, $(0, 1, 0, \dots, 0)^T$, and so on, where T denotes the transpose operation. Because of being multiplied by the successive TMs, the directions of the initial vectors change. The Lyapunov exponents are then the logarithm of the trace of the matrix, $\mathbf{V} = [\mathbf{T}(\mathbf{T}^T)^{1/2n}]$, where, $\mathbf{T} = \mathbf{T}_n \mathbf{T}_{n-1} \dots \mathbf{T}_1$. Then, the direction that corresponds to the largest Lyapunov is the direction of the eigenvector that corresponds to the largest eigenvalue of the matrix \mathbf{V} .

However, after a few steps, the information about all the Lyapunov exponents but the largest one will be lost in the numerical noise. To avoid this difficulty we implemented the Gram-Schmidt (GS) orthogonalization after every two steps of the TM iterations. The number of steps after which the GS orthogonalization should be applied depends on the model, and may actually be estimated.^{22,23} For example, in the computations for the Anderson model the GS orthogonalization is applied after every 10 steps.

IV. DENSITY OF STATES

As mentioned above, a useful quantity for characterizing propagation of elastic waves in a disordered solid is the vibrational density of states (DOS) $\mathcal{N}(\omega)$. The usefulness of $\mathcal{N}(\omega)$ is due to its dependence on the strength of the disorder and, therefore, it is an important characteristic of heterogeneous media. To compute the DOS we used the forced-oscillator (FO) method,^{5,24,25} which

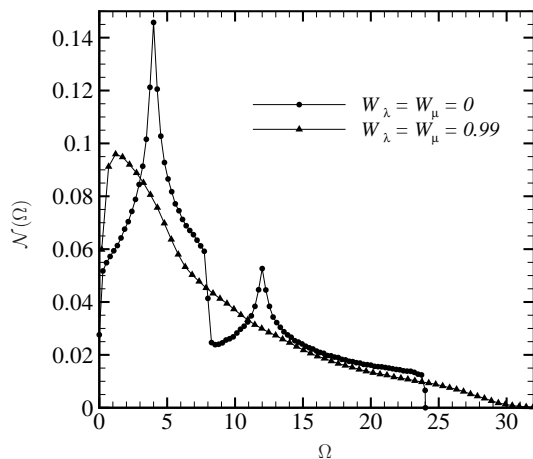


FIG. 2: Density of states $\mathcal{N}(\Omega)$ of the 2D model, calculated with a computational grid of size 1000×1000 .

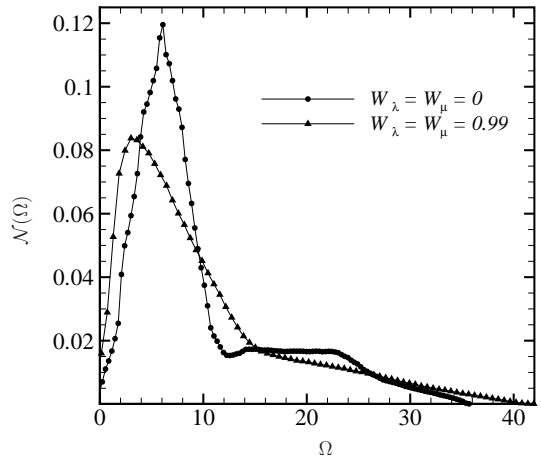


FIG. 3: Density of states $\mathcal{N}(\Omega)$ of the 3D model, calculated with a computational grid of size $100 \times 100 \times 100$. The curves are guide to the eye.

made it is possible to use computational grids of size, $10^3 \times 10^3$ in 2D and, $10^2 \times 10^2 \times 10^2$ in 3D. The FO method is based on the principle that a complex mechanical system, driven by a periodic external force of frequency Ω , responds with a large amplitude in those eigenmodes that are close to Ω .

Let us point out that, although computing the DOS is not directly crucial for the search for a mobility edge, it is, nevertheless, a very useful quantity to calculate. For example, the DOS helps one to identify the allowed range of the frequencies (see Figs. 2 and 3 below), with the help of which the computations are carried out more efficiently for the mobility edge search in the frequency range.

V. RESULTS AND DISCUSSIONS

In what follows, we describe the results of the numerical simulations, and discuss their implications.

A. Density of states

For an elastic medium in which wave propagation is described by Eq. (1), all the eigenvalues of the matrix \mathbf{H} are positive. As a result, the system undergoes an asymmetric broadening of the band of the allowed frequencies (energies). In Fig. 2 we present the DOS $\mathcal{N}(\Omega)$ for the 2D ordered, as well as random, media. There are two peaks corresponding to two branches of the characteristic equation, i.e., the transverse and longitudinal modes. The two modes propagate independently in 2D and, therefore, each branch has the same DOS as that of the 2D Anderson model. As is well known, without disorder the DOS has cusps in 2D, containing some special points that are usually called the von Hove singularities, at which the DOS is nondifferentiable. As Fig. 2 indicates, by adding randomness to the Lamé coefficients of the medium, the von Hove singularities disappear and a band tail appears in the upper band edge.

TABLE I: The rescaled Lyapunov exponents $M\gamma_m$ (inverse of the rescaled localization length) of the 2D model and the corresponding errors. n is the index number of γ_m . The results are for $M = 6$, $L = 10^5$, $\Omega = 1$, $W_\lambda = W_\mu = 0.99$, and $\lambda_0 = \mu_0 = 1.0$. The Gram-Schmidt orthogonalization was implemented after every two steps.

n	$M\gamma_m$	error	n	$M\gamma_m$	error
1	15.421216	0.018	13	-0.146944	0.007
2	13.044478	0.015	14	-0.384629	0.007
3	10.675876	0.012	15	-0.769397	0.008
4	8.019660	0.010	16	-1.404398	0.009
5	6.411892	0.009	17	-2.559604	0.010
6	5.138542	0.008	18	-3.831230	0.010
7	3.831297	0.008	19	-5.138530	0.009
8	2.559524	0.008	20	-6.411741	0.010
9	1.404456	0.007	21	-8.019935	0.012
10	0.769496	0.006	22	-10.675919	0.014
11	0.384616	0.006	23	-13.044517	0.016
12	0.146903	0.006	24	-15.421134	0.018

Figure 3 presents the DOS $\mathcal{N}(\Omega)$ for the corresponding 3D media. The results seem similar to those for the 2D media, although the cusps do not appear as sharp. Once again, disorder in the form of the spatial distributions of the Lamé coefficients make the DOS smooth. We show in the next section, however, that propagation of elastic waves in the the 2D and 3D media is different, if we study its localization properties.

B. Lyapunov exponent and localization length

The computed Lyapunov exponents γ_m are presented in Table I for $\Omega = 1$. They occur in pairs, $(\gamma, -\gamma)$, which indicate the symplectic symmetry of the TMs. We found that after every two steps the GS orthogonalization must be implemented. The estimated errors shown were computed as follows. After each GS orthogonalization the length d_α is computed for normalizing the evolving vector \mathbf{Z}_n in Eq. (5), which then results in a sequence $\{d_\alpha\}$. The average of the logarithm of such lengths yields the LE,

$$\gamma = \frac{1}{mp} \sum_{\alpha=1}^N \ln(d_\alpha), \quad (6)$$

after normalizing the vectors p times, with m being the steps of GS orthogonalization (here $m = 2$). Moreover, the error in estimating γ (see Table I) is given by,²⁶

$$\frac{\Delta\gamma}{\gamma} = \frac{1}{\sqrt{p}} \frac{\sqrt{\langle(\ln d_\alpha)^2\rangle - \langle\ln d_\alpha\rangle^2}}{\langle\ln d_\alpha\rangle}, \quad (7)$$

where the brackets indicate averaging over the sequence of $\{d_\alpha\}$. γ is a self-averaged quantity,²⁶ and the error of its estimates approaches zero as p increases. Note that, not all the Lyapunov exponents are independent; we only need to compute the first N of them. The smallest positive Lyapunov exponent, γ_m , corresponds to the localization length that we wish to determine and study.

Figure 4 presents the inverse of the scaled localization length, $\Lambda = (M\gamma_m)^{-1}$, in the 2D media as a function of $\Omega = \omega^2$ for the disorder parameters, $W_\lambda = W_\mu = 0.99$ and $\lambda_0 = \mu_0 = 1.0$, and several M , the width of the strips used in the TM computations. The calculations were carried out with an accuracy of 0.1%. At first glance, it appears that Λ decreases by increasing the width, implying that it vanishes in the thermodynamic limit and, therefore, all the states are localized in the 2D disordered media that we studied, up to the frequencies that were considered.

However, a closer inspection of Fig. 4 indicates an intriguing possibility. It appears that for $\Omega > 10$, Λ^{-1} exhibits an M -dependence, whereas for $\Omega < 10$ the dependence on M is weak, if it exists at all. The difference indicates that the possibility of the existence of a mobility

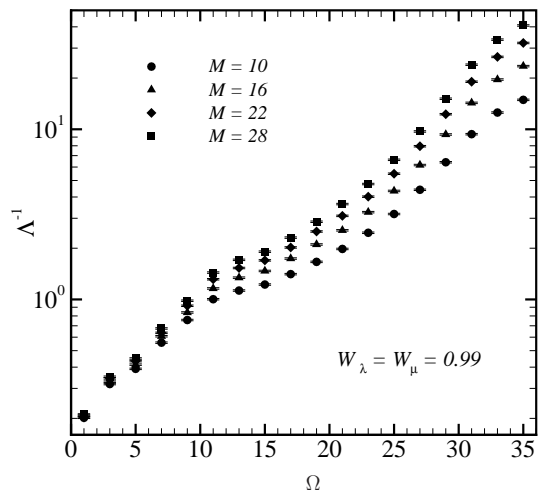


FIG. 4: Inverse of the scaled localization length Λ of the 2D model, obtained with an accuracy of 0.1%.

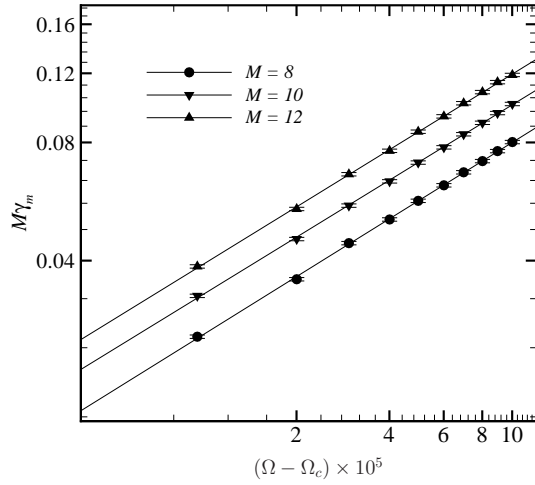


FIG. 5: Inverse of the scaled localization length Λ of the $M \times L$ strips with $W_\mu = 0$ and $W_\lambda = 0.99$. The results were obtained with an accuracy of 0.1%.

edge cannot be completely ruled out in such 2D media. If mobility edge does exist, it would then be consistent with the prediction of the RG calculations¹² for the 2D media, which did predict the existence of such a mobility edge in 2D. We shall come back to this point shortly.²⁸

Next, we consider a special case in which the shear modulus μ is constant, but the bulk modulus λ is distributed randomly. Such a limiting case is of interest, because a 2D medium of this type does have a band of extended states. It is straightforward to show that, for a constant μ , Eqs. (A1) and (A2) have a solution that propagates without any scattering which, in fact, represents plane waves with transverse polarization, for which the dispersion relation is given by

$$\Omega = 4 - 2 \cos(k_x) - 2 \cos(k_y), \quad (8)$$

where $\mathbf{k} = (k_x, k_y)$ is the wave vector. The dispersion relation (6) has a frequency band in the range, $0 < \Omega < 8$, in which we find a zero Lyapunov exponent, implying infinite localization length and, therefore, extended states. Moreover, there is a mobility edge at $\Omega_c = 8$, and as $\Omega \rightarrow \Omega_c^+$, one has

$$\gamma_m \propto (\Omega - \Omega_c)^{\nu_T}. \quad (9)$$

Figure 5 presents the frequency-dependence of the rescaled Lyapunov exponent, $M\gamma_m$, near $\Omega_c = 8$ for several strip widths M . The data are well-fitted by the power law (7), yielding the estimate, $\nu_T \simeq 0.496 \pm 0.003$, independent of the width M .

In 3D media, however, the Lyapunov exponent behaves differently. Figure 6 displays the results for the inverse of the (rescaled) localization length Λ^{-1} for the same disorder parameters as those in the 2D media. The results for all values of the width M of the 3D bars (used in the TM computations) intersect one another at a particular critical frequency Ω_c . For $\Omega < \Omega_c$ the rescaled Lyapunov

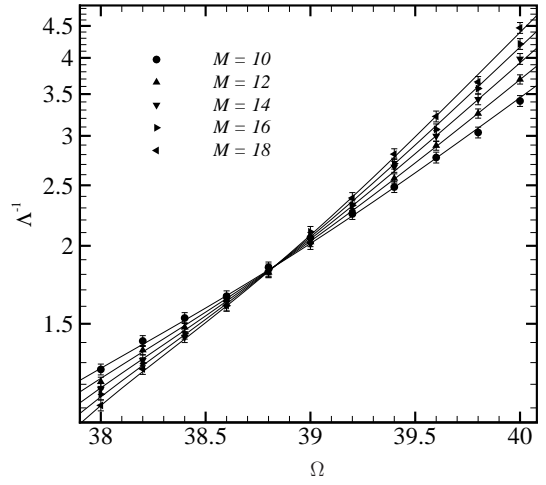


FIG. 6: Inverse of the scaled localization length Λ of the 3D model for $W_\mu = W_\lambda = 0.99$, obtained with an accuracy of 2%. Solid curves represent the fit of the data to Eq. (10).

exponent decreases with increasing M , i.e., one has extended states.

To obtain better understanding of the localization properties, we analyze the numerical data for the localization length. The inverse of the (rescaled) localization length, Λ^{-1} is a function of a single scaling variable, and is expressed as

$$\Lambda^{-1} = F(\chi M^{1/\nu}) = \sum_{i=0}^n a_i \chi^i M^{i/\nu}, \quad (10)$$

where ν is the localization length exponent, $\Lambda \sim (\Omega - \Omega_c)^{-\nu}$ and χ is the scaling variable. a_0 represents the critical value of Λ_c^{-1} . The absolute scale of the argument in Eq. (10) is arbitrary; we fix the coefficients by setting $a_1 = 1$. The scaling variable χ is then expanded as a function of the reduced frequency Ω_r ,

$$\chi = \sum_{i=1}^m b_i \Omega_r^i, \quad (11)$$

$$\Omega_r = (\Omega - \Omega_c) / \Omega_c. \quad (12)$$

For a large enough system, it is not necessary to keep the higher order terms of Eqs. (10) and (11) in the critical region near Ω_c . Here, however, due to the relatively small sizes of the 3D bars that we used in the TM simulations, we need some of the leading order terms in order to obtain accurate fit of the data. If the number of terms in the expansions (10) and (11) are, respectively, selected to be, $n = 3$ and $m = 2$, we obtain an accurate fit of the data with

$$\nu \simeq 1.89 \pm 0.17, \quad \Lambda_c^{-1} \simeq 1.84 \pm 0.06, \quad \Omega_c \simeq 38.82 \pm 0.06, \quad (13)$$

where the estimated errors are with 95% confidence.

The above estimate of the critical exponent ν is different from the estimate²⁹ of the corresponding exponent for the Anderson model of electron localization,

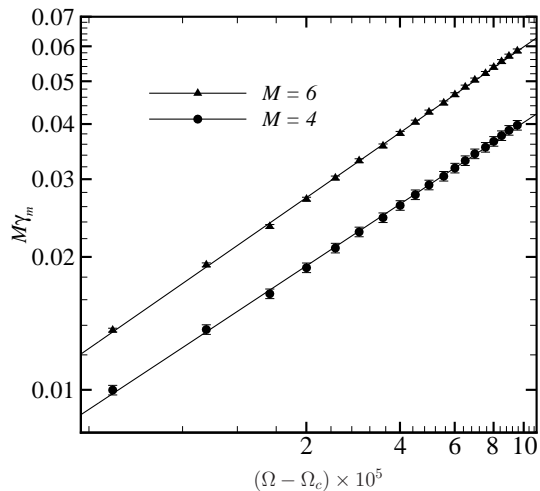


FIG. 7: Inverse of the scaled localization length Λ of the $M \times M \times L$ bars with $W_\mu = 0$ and $W_\lambda = 0.99$. The results were obtained with an accuracy of 0.1%.

$\nu \simeq 1.57 \pm 0.01$. It is also much larger than $\nu = 3/2$, which was recently derived³⁰ based on a semiclassical theory for the 3D Anderson model of electron localization. The important implication of the difference is that, the localization-delocalization transition for elastic waves in the 3D disordered media that we study belongs to a universality class different from that of the Anderson model. The difference is presumably related to the different symmetries of the underlying Hamiltonians for the two phenomena. We note, however, that, due to the relatively large estimated errors of ν for the elastic waves, we cannot completely rule out the possibility that the two models belong to the same universality class.

Similar to the 2D media, the special limit in which the shear modulus μ is constant, but the bulk modulus λ varies spatially, may also be studied in 3D media. In this case the transverse plane waves have a dispersion relation given by

$$\Omega = 6 - 2 \cos(k_x) - 2 \cos(k_y) - 2 \cos(k_z). \quad (14)$$

Therefore, the frequency band of such waves is the interval $0 < \Omega < 12$. Figure 7 presents frequency-dependence of the rescaled minimum Lyapunov exponent, γ_m . The results indicate that, near the mobility edge $\Omega_c = 12$, γ_m follows the same type of power law as in the 2D media, with an exponent, $\nu_T \simeq 0.481 \pm 0.004$, very close to that estimated for the 2D media and roughly equal to $1/2$.

C. Statistics of energy levels

An important aspect of the symmetry of any Hamiltonian is its level-spacing statistics, which have been studied extensively by the theory of random matrices. The statistics of the level spacings s for the elastic waves indicate that, in the localized regime where the localization length is small compared to the medium's linear size, the levels are uncorrelated and, therefore, they follow a

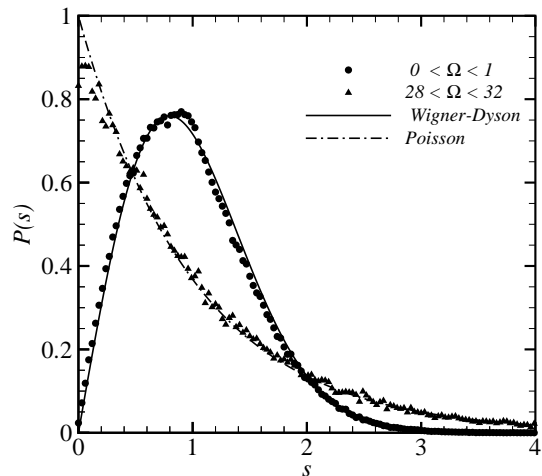


FIG. 8: Distribution of the level spacings for 10^3 realizations of 2D media of size 50^2 for two frequency intervals. The results for the high frequency interval follows the Poisson statistics, while the results for the low-frequency interval follows the statistics of the Gaussian orthonormal ensemble.

Poisson distribution. Figure 8 presents such energy-level statistics for the 2D media for two frequency ranges. The parameter s is defined by

$$s = \frac{\Omega_{n+1} - \Omega_n}{\langle \Omega_{n+1} - \Omega_n \rangle}.$$

The results, shown in Fig. 8, were obtained by exact diagonalization of 1000 realizations of the disorder using 50×50 computational grids. In the interval $28 < \Omega < 32$ the statistics do follow the Poisson distribution. For low frequencies in the interval $0 < \Omega < 1$, however, the data are well-fitted by the Wigner-Dyson distribution. Indeed, the Wigner-Dyson and Poisson distributions represent

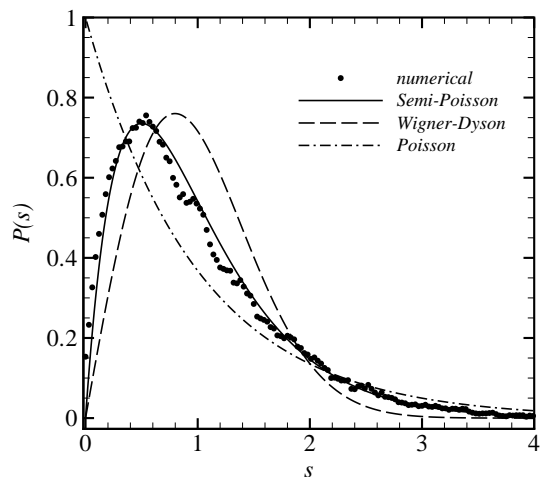


FIG. 9: Distribution $P(s)$ of the level spacings for 120 realizations of the 3D media of size 30^3 for the frequency interval $36 < \Omega < 40$, near the critical frequency Ω_c . $P(s)$ is nearly semi-Poisson.

the statistics for certain limits that are attained in the thermodynamic limit. In fact, the Wigner-Dyson distribution, which describes the statistics of the level spacings in the low frequency limit, will approach the Poisson distribution by increasing the system size,³¹ if there is no true mobility edge in two dimensions.

At the localization-delocalization transition point in 3D, the distribution function of the level spacings is independent of the system's size, and is represented by the semi-Poisson distribution,³² $P(s) = 4s \exp(-2s)$. Figure 9 presents the distribution function of the level spacings in the 3D model for the frequencies near the critical frequency Ω_c , obtained by using 120 realizations of the disorder in $30 \times 30 \times 30$ computational grids. The results indicate clearly that the distribution is essentially semi-Poisson.

D. Comparison with the predictions of the dynamic renormalization

In a previous paper¹² we studied localization of elastic waves in 2D heterogeneous solids with randomly distributed Lamé coefficients, as well as those with long-range correlations with a power-law correlation function, characterized by an exponent ρ . The Martin-Siggia-Rose method¹³ was used, and the one-loop RG equations for the the coupling constants were derived in the limit of low frequencies (long wavelengths). We found, in particular, that for $\rho < 1$ there is a region of the coupling constants space in which the RG flows are toward the Gaussian fixed point, implying that the disorder is irrelevant and, therefore, the waves are delocalized. In the rest of the disorder space the elastic waves were found to be localized.

The numerical results for the 2D media presented in the present paper, when the two Lamé coefficients are spatially distributed, do not seem to indicate the existence of any extended states. If this is true, then the discrepancy between the numerical simulations and the RG predictions may be due to the fact that, the RG results are valid only in the low-frequency limit, and the smallest frequencies that we considered in the present paper may be larger than those for which the RG results are valid.

At the same time, as discussed above, the M -dependence of the inverse (rescaled) localization length Λ^{-1} for a range of frequencies $\Omega > 10$, and its absence for $\Omega < 10$, open up the possibility that, consistent with the RG predictions, a mobility edge does exist in the 2D media that we study. In that case, we would have further evidence that question of localization of elastic waves in heterogeneous media is fundamentally different from that of Anderson localization of electrons. This is clearly an issue that deserves further study. Work in this direction is in progress.

VI. SUMMARY

We studied the localization properties of elastic waves in a disordered elastic medium in both two and three di-

mensions. We found that if the disorder, in the form of spatially-varying Lamé coefficients, is broadly distributed, it may lead to the localization of all the states in the 2D media, although there is some evidence that a mobility edge might exist in such media. The same disorder strength cannot, however, localize all the states in the 3D media. There is a mobility edge in 3D, near which the (rescaled) localization length follows a power law, $\Lambda \sim (\Omega - \Omega_c)^{-\nu}$. Using extensive numerical simulations and a scaling analysis, the estimated ν was found to be different from that of the Anderson model of electron localization. The statistics of the energy levels indicated, however, that in the extended regime it is generally the Gaussian orthogonal ensemble statistics¹¹ that govern the energy levels. In the limit in which the shear modulus is constant but the bulk modulus varies spatially, there is a mobility edge even in 2D, for which the associated critical exponent ν_T for the power-law behavior of the localization length near the edge was also computed. We found for both the 2D and 3D media that, $\nu_T \simeq 1/2$.

APPENDIX: THE FINITE-DIFFERENCE EQUATIONS

We list the discretized equations that govern the displacements of the grid points during propagation of elastic waves in the 2D and 3D computational grids.

Two-dimensional media

$$-m\omega^2 u = D_x[(\lambda + 2\mu)D_x u] + D_y(\mu D_y u) + D_y(\mu D_x w) + D_x(\lambda D_y w)|_{i,j}, \quad (\text{A.1})$$

$$-m\omega^2 w = D_y[(\lambda + 2\mu)D_y w] + D_x(\mu D_x w) + D_x(\mu D_y u) + D_y(\lambda D_x u)|_{i+\frac{1}{2},j+\frac{1}{2}}. \quad (\text{A.2})$$

where

$$D_x f(i, j) = \frac{1}{h} \left[f(i + \frac{1}{2}, j) - f(i - \frac{1}{2}, j) \right], \quad (\text{A.3})$$

$$D_y f(i, j) = \frac{1}{h} \left[f(i, j + \frac{1}{2}) - f(i, j - \frac{1}{2}) \right]. \quad (\text{A.4})$$

Three-dimensional media

$$-m\omega^2 u = D_x[(\lambda + 2\mu)D_x u] + D_y(\mu D_y u) + D_z(\mu D_z u) + D_y(\mu D_x w) + D_x(\lambda D_y w) + D_x(\mu D_z v) + D_z(\lambda D_x v)|_{i,j,k}, \quad (\text{A.5})$$

$$-m\omega^2 w = D_y[(\lambda + 2\mu)D_y w] + D_x(\mu D_x w) + D_y(\mu D_y w) + D_x(\mu D_y u) + D_y(\lambda D_x u) + D_y(\mu D_z v) + D_z(\lambda D_y v)|_{i+\frac{1}{2},j+\frac{1}{2},k}, \quad (\text{A.6})$$

$$-m\omega^2 v = D_z[(\lambda + 2\mu)D_z v] + D_x(\mu D_x v) + D_y(\mu D_y v) + D_z(\mu D_x u) + D_x(\lambda D_z u) + D_z(\mu D_y w) + D_y(\lambda D_z w)|_{i+\frac{1}{2},j,k+\frac{1}{2}}. \quad (\text{A.7})$$

where

$$D_x f(i, j, k) = \frac{1}{h} \left[f\left(i + \frac{1}{2}, j, k\right) - f\left(i - \frac{1}{2}, j, k\right) \right], \quad (\text{A.8})$$

$$D_y f(i, j, k) = \frac{1}{h} \left[f\left(i, j + \frac{1}{2}, k\right) - f\left(i, j - \frac{1}{2}, k\right) \right], \quad (\text{A.9})$$

$$D_z f(i, j, k) = \frac{1}{h} \left[f\left(i, j, k + \frac{1}{2}\right) - f\left(i, j, k - \frac{1}{2}\right) \right]. \quad (\text{A.10})$$

We took $h = 1$.

*moe@iran.usc.edu

- ¹A. Ishimaru, *Wave Propagation and Scattering in Random Media* (Academic, New York, 1978).
- ²N. Bleistein, J. K. Cohen, and J. W. Stockwell, Jr., *Mathematics of Multidimensional Seismic Imaging, Migration, and Inversion* (Springer, New York, 2001).
- ³A. V. Granato and K. Lücke, in *Physical Acoustics*, edited by W. P. Mason (Academic, New York, 1966), Vol. 4a.
- ⁴M. R. Rahimi Tabar, M. Sahimi, F. Ghasemi, K. Kaviani, M. Allamehzadeh, J. Peinke, M. Mokhtari, M. Vesaghi, M. D. Nirry, A. Bahraminasab, S. Tabatabai, S. Fayyazbakhsh, and M. Akbari, in *Modelling Critical and Catastrophic Phenomena in Geoscience*, edited by P. Bhattacharya and B. K. Chakrabarti (Springer, Berlin, 2006); P. Manshoor, S. Saberi, M. Sahimi, J. Peinke, A. F. Pacheco, and M. R. Rahimi Tabar (unpublished).
- ⁵M. Sahimi, *Heterogeneous Materials I & II* (Springer, New York, 2003).
- ⁶See, for example, J. B. Keller, Proc. Symp. Appl. Math. **16**, 145 (1964); T. Yamashita, Pure Appl. Geophys. **132**, 545 (1990).
- ⁷J. E. Gubernatis, E. Domany, and J. A. Krumhansl, J. Appl. Phys. **48**, 2804 (1977).
- ⁸E. Larose, L. Margerin, B. A. van Tiggelen, and M. Campillo, Phys. Rev. Lett. **93**, 048501 (2004).
- ⁹P. W. Anderson, Phys. Rev. **109**, 1492 (1958).
- ¹⁰E. P. Wigner, Ann. Math. **53**, 36 (1951); F. J. Dyson, J. Math. Phys. **3**, 140 (1962).
- ¹¹M. L. Mehta, *Random Matrices* (Academic, Boston, 1991).
- ¹²R. Sepehrinia, A. Bahraminasab, M. Sahimi, and M. R. Rahimi Tabar, Phys. Rev. B **77**, 014203 (2008).
- ¹³P. C. Martin, E. G. Siggia, and H. A. Rose, Phys. Rev. A **8**, 423 (1973).
- ¹⁴P. H. Song and D. S. Kim, Phys. Rev. B **54**, R2288 (1996).
- ¹⁵Y. Akita and T. Ohtsuki, J. Phys. Soc. Jpn. **67**, 2954 (1998).
- ¹⁶J. J. Ludlam, S. N. Taraskin, and S. R. Elliot, Phys. Rev. B **67**, 132203 (2003).
- ¹⁷T.-K. Hong and B. L. N. Kennett, Geophys. J. Int. **150**, 610 (2002); *ibid.* **154**, 483 (2003).
- ¹⁸Y. Q. Zeng and Q. H. Liu, J. Acous. Soc. Amer. **109**, 2571 (2001).
- ¹⁹T. Bohlen, Comput. Geosci. **28**, 887 (2002).
- ²⁰H. A. Friis, T. A. Johansen, M. Haverdaen, H. Munthe-Kaas, and A. Drottning, Appl. Numer. Math. **39**, 151 (2001).
- ²¹M. Sahimi and S. M. Vaez Allaei, Comput. Sci. Eng. **10** (No. 3), 66 (2008).
- ²²A. MacKinnon and B. Kramer, Z. Phys. B **53**, 1 (1983).
- ²³J. L. Pichard and G. Sarma, J. Phys. C **14** L127 (1981).
- ²⁴M. L. Williams and H. J. Maris, Phys. Rev. B **31**, 4508 (1985).
- ²⁵K. Yakubo and T. Nakayama, Phys. Rev. B **40**, 517 (1989); K. Yakubo, T. Nakayama, and H. J. Maris, J. Phys. Soc. Jpn. **60**, 3249 (1990); K. Yakubo, K. Takasugi, and T. Nakayama, *ibid.* **59**, 1909 (1990); T. Nakayama and K. Yakubo, Phys. Rep. **349**, 239 (2001).
- ²⁶R. Sepehrinia, M. D. Nirry, N. Bozorg, M. R. Rahimi Tabar, and M. Sahimi, Phys. Rev. B **77**, 104202 (2008).
- ²⁷P. Markos, [arXiv:cond-mat/0609580v1](https://arxiv.org/abs/cond-mat/0609580v1)
- ²⁸The subject remains controversial. See, for example, P. Markos and C. M. Soukoulis, Phys. Rev. B **71**, 054201 (2005).
- ²⁹K. Slevin and T. Ohtsuki, Phys. Rev. Lett. **82**, 382 (1999).
- ³⁰A. M. García-García, Phys. Rev. Lett. **100**, 076404 (2008).
- ³¹I. Kh. Zharekeshev, M. Batsch, and B. Kramer, Europhys. Lett. **34**, 587 (1996).

³²D. Braun, G. Montambaux, and M. Pascaud, Phys. Rev. Lett. **81**, 1062 (1998); E. B. Bogomolny, U. Gerland, and C. Schmit, Phys. Rev. E. **59**, 1315

(1999); S. N. Evangelou, J. Phys. A **38**, 363 (2005).